

# A Fenton Mechanism and an Oxochromium(IV) Intermediate in Reactions of the Hydroperoxochromium(III) Ion

Wei-Dong Wang, Andreja Bakac,\* and James H. Espenson\*

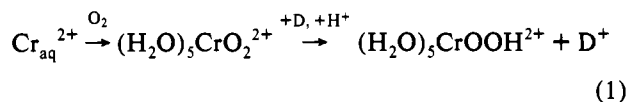
Department of Chemistry, Iowa State University, Ames, Iowa 50011

Received September 11, 1992

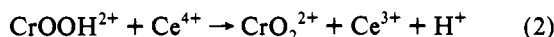
The covalently bound hydroperoxo complex  $(\text{H}_2\text{O})_5\text{CrOOH}^{2+}$  is reduced by  $\text{Fe}^{2+}$  in aqueous solution by a Fenton mechanism. The reaction is second-order, with  $k_{298} = 48.4 \text{ L mol}^{-1} \text{ s}^{-1}$  ( $\Delta H^\ddagger = 30.0 \pm 0.7 \text{ kJ mol}^{-1}$  and  $\Delta S^\ddagger = -110 \pm 2 \text{ J mol}^{-1} \text{ K}^{-1}$ ). These values are close to those for the  $\text{H}_2\text{O}_2/\text{Fe}^{2+}$  reaction. In the Fenton mechanism, if it applies to the reaction between  $\text{CrOOH}^{2+}$  and  $\text{Fe}^{2+}$ ,  $\text{CrO}^{2+}$  would be an intermediate. It was identified by trapping with  $\text{HC}_2\text{O}_4^-$  and with a water-soluble phenol, [2-methyl-2-(3,5-di-*tert*-butyl-4-hydroxyphenyl)propyl]ammonium chloride. The new products formed, and their yields, support a scheme in which  $\text{CrO}^{2+}$  occurs as an intermediate. This could be tested directly, since the properties and reactivity of this species are independently known. The reaction of  $\text{CrO}^{2+}$  with  $\text{Fe}^{2+}$  has  $k = 3.8 \times 10^3 \text{ L mol}^{-1} \text{ s}^{-1}$ ,  $\Delta H^\ddagger = 28.3 \pm 1.8 \text{ kJ mol}^{-1}$ , and  $\Delta S^\ddagger = -81 \pm 2 \text{ J mol}^{-1} \text{ K}^{-1}$ .

## Introduction

The reaction of  $\text{Cr}_{\text{aq}}^{2+}$  with  $\text{O}_2$  produces the superoxochromium(III) ion,  $(\text{H}_2\text{O})_5\text{CrO}_2^{2+}$ , as the first observable intermediate.<sup>1,2</sup> Our recent resonance Raman study supports an end-on geometry for this molecule.<sup>1d</sup> The reaction of  $(\text{H}_2\text{O})_5\text{CrO}_2^{2+}$  with certain one-electron donors yields a species for which we proposed an end-on hydroperoxo structure,  $(\text{H}_2\text{O})_5\text{CrOOH}^{2+}$  (henceforth  $\text{CrOOH}^{2+}$ ) (eq 1). Species D in eq 1 represents



outer-sphere reductants, such as  $\text{Ru}(\text{NH}_3)_6^{2+}$  or  $\text{V}(\text{H}_2\text{O})_6^{2+}$ .<sup>1c,2</sup> Some of the evidence supporting the end-on structure for  $\text{CrOOH}^{2+}$  comes from the reversibility of the redox process: the one-electron oxidation of the purported  $\text{CrOOH}^{2+}$  by  $\text{Ce}(\text{IV})$  results in a clean recovery of  $\text{CrO}_2^{2+}$  in >75% yield.<sup>2</sup> This reaction resembles the oxidation of hydrogen peroxide and alkyl hydroperoxides by  $\text{Ce}(\text{IV})$  as shown in eq 3.<sup>3</sup>



Additional evidence concerning the structure of  $\text{CrOOH}^{2+}$  is provided by the kinetic results obtained in this work (see later). The long-lived  $\text{CrOOH}^{2+}$  (half-life of approximately 15 min under typical conditions) and several hydroperoxocobalt compounds<sup>4</sup> are the only known examples of metal hydroperoxides in aqueous solution.

Considerable data on the reduction of hydrogen peroxide and alkyl hydroperoxides by transition metal ions have been reported,<sup>5,6</sup> but very little is known about the reactivity of transition-metal

hydroperoxides,  $\text{L}_n\text{MOOH}^{n+}$ .<sup>4,7</sup> The long lifetime of  $\text{CrOOH}^{2+}$  has provided us with an opportunity to compare directly the reactivity of a metal hydroperoxide with that of  $\text{H}_2\text{O}_2$  and  $\text{ROOH}$ . Also, if we find a pattern to the chemistry that is typical of free peroxides, it would lend additional support to our structural assignment for the peroxochromium ion as an end-on species.

The present kinetic study for the reaction of  $\text{Fe}^{2+}$  with  $\text{CrOOH}^{2+}$  was undertaken to examine the mechanism of reactions of a peroxide anion covalently attached to a chromium(III) center. Specifically we wanted to know whether coordination to  $\text{Cr}^{3+}$  deactivates the peroxide and whether  $\text{CrO}^{2+}$  is involved as intermediate in these reactions.

## Experimental Section

**Reagents.**  $[\text{Ru}(\text{NH}_3)_6]\text{Cl}_3$  was purchased from Alfa and used without purification. Solutions of  $[\text{Ru}(\text{NH}_3)_6]^{2+}$  were prepared by reduction of  $[\text{Ru}(\text{NH}_3)_6]\text{Cl}_3$  in  $\text{H}_2\text{O}$  with  $\text{Zn}/\text{Hg}$  and used within 4 h. The concentration of  $\text{Ru}(\text{II})$  was determined spectrophotometrically ( $\epsilon_{275\text{nm}} = 620 \text{ L mol}^{-1} \text{ cm}^{-1}$ ).<sup>8</sup> Solutions of  $\text{Fe}^{2+}$  were prepared by reduction of  $\text{Fe}(\text{ClO}_4)_3$  with  $\text{Zn}/\text{Hg}$  in 0.1 M  $\text{HClO}_4$  solution under Ar. The concentrations of  $\text{Fe}^{3+}$  were determined spectrophotometrically ( $\epsilon_{240\text{nm}} = 4160 \text{ L mol}^{-1} \text{ cm}^{-1}$ ).<sup>9</sup>  $\text{Cr}(\text{ClO}_4)_3 \cdot n\text{H}_2\text{O}$  was prepared by reduction of  $\text{CrO}_3$  by  $\text{H}_2\text{O}_2$  in dilute perchloric acid and recrystallized twice. The concentration of  $\text{Cr}^{3+}$  was determined spectrophotometrically ( $\epsilon_{408\text{nm}} = 15.6 \text{ L mol}^{-1} \text{ cm}^{-1}$ ). Solutions of  $\text{Cr}^{2+}$  were prepared by reduction of a known amount of  $\text{Cr}^{3+}$  with  $\text{Zn}/\text{Hg}$  in 0.10 M  $\text{H}^+$ .  $\text{LiClO}_4$  was prepared from  $\text{Li}_2\text{CO}_3$  and  $\text{HClO}_4$  and recrystallized three times. Solutions of  $\text{LiClO}_4$  were standardized by ion exchange on Dowex 50W-X4 in acid form, followed by the titration of the replaced  $\text{H}^+$  by a standard solution of  $\text{NaOH}$ . Dilute solutions of  $\text{H}_2\text{O}_2$  were standardized iodometrically. Solutions of  $\text{CrOOH}^{2+}$  were prepared by reduction of  $\text{CrO}_2^{2+}$  with  $\text{Ru}(\text{NH}_3)_6^{2+}$ .<sup>2</sup> The concentration of  $\text{CrOOH}^{2+}$  was determined by adding an excess of  $\text{NaI}$  to the solution and measuring the absorbance of  $\text{I}_3^-$  at

- (1) (a) Bruhn, S. L.; Bakac, A.; Espenson, J. H. *Inorg. Chem.* **1986**, *25*, 535. (b) Brynildson, M. E.; Bakac, A.; Espenson, J. H. *J. Am. Chem. Soc.* **1987**, *109*, 4579. (c) Brynildson, M. E.; Bakac, A.; Espenson, J. H. *Inorg. Chem.* **1988**, *27*, 2592. (d) Scott, S. L.; Bakac, A.; Espenson, J. H.; Rodgers, K. L. Submitted for publication. (2) Scott, S. L.; Bakac, A.; Espenson, J. H. *Inorg. Chem.* **1991**, *30*, 4112. (3) Kochi, J. K. *Organometallic Mechanisms and Catalysis*; Academic Press: New York, 1978; pp 60–68. (4) (a) Wong, C.-L.; Endicott, J. F. *Inorg. Chem.* **1981**, *20*, 2233. (b) Geiger, T.; Anson, F. C. *J. Am. Chem. Soc.* **1981**, *103*, 7489. (c) Gubelmann, M. H.; Ruttimann, S.; Bocquet, B.; Williams, A. F. *Helv. Chim. Acta* **1990**, *73*, 1219.

- (5) (a) Hyde, M. R.; Espenson, J. H. *J. Am. Chem. Soc.* **1976**, *98*, 4463. (b) Espenson, J. H.; Martin, A. H. *J. Am. Chem. Soc.* **1977**, *99*, 5953. (c) Bakac, A.; Espenson, J. H. *Inorg. Chem.* **1983**, *22*, 779. (d) Bakac, A.; Espenson, J. H. *J. Am. Chem. Soc.* **1986**, *108*, 713. (e) Kim, H. P.; Espenson, J. H.; Bakac, A. *Inorg. Chem.* **1987**, *26*, 4090. (f) Masarwa, M.; Cohen, H.; Meyerstein, D.; Hickman, D. L.; Bakac, A.; Espenson, J. H. *J. Am. Chem. Soc.* **1988**, *110*, 4293. (g) Sadler, N.; Scott, S. L.; Bakac, A.; Espenson, J. H.; Ram, M. S. *Inorg. Chem.* **1989**, *28*, 3951. (6) (a) Kochi, J. K. *Rec. Chem. Prog.* **1966**, *27*, 207. (b) Sheldon, R. A.; Kochi, J. K. *Metal Catalyzed Oxidations of Organic Compounds*; Academic Press: New York, 1991; pp 33–43. (c) Rush, J. D.; Bielski, B. H. *J. Inorg. Chem.* **1985**, *24*, 4282. (7) (a) Michelin, R. A.; Ros, R.; Strukul, G. *Inorg. Chim. Acta* **1979**, *37*, L491. (b) Roberts, H. L.; Symes, W. R. *J. Chem. Soc. A* **1968**, 1450. (8) Armor, J. N.; Scheidegger, H. A.; Taube, H. *J. Am. Chem. Soc.* **1968**, *90*, 5928. (9) Carlyle, D. W.; Espenson, J. H. *Inorg. Chem.* **1967**, *6*, 1370.

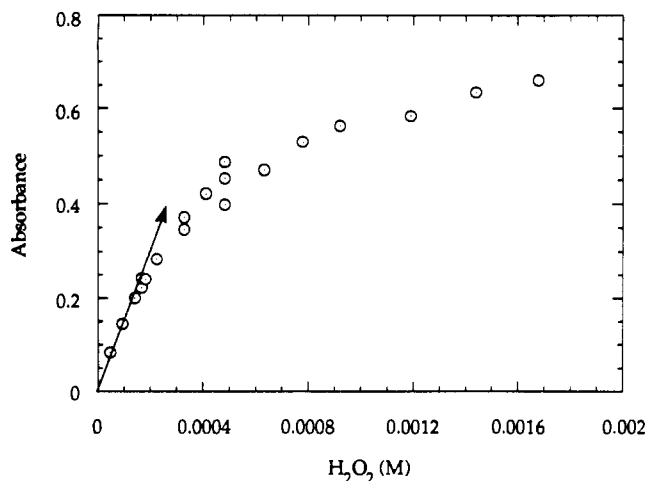
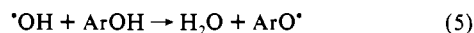
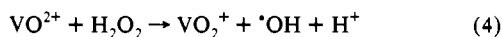


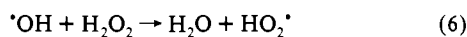
**Figure 1.** Plot of  $\Delta(\text{absorbance})$  versus  $[\text{H}_2\text{O}_2]$  for the determination of the molar absorption coefficient of  $\text{ArO}^*$ . Conditions:  $\lambda = 400 \text{ nm}$ ,  $[\text{ArOH}] = 3 \text{ mM}$ ,  $[\text{VO}^{2+}] = 7.6 \text{ mM}$ ,  $[\text{HClO}_4] = 0.1 \text{ M}$ .

350 nm ( $\epsilon_{350\text{nm}} = 2.5 \times 10^4 \text{ L mol}^{-1} \text{ cm}^{-1}$ ).<sup>10</sup> Sodium oxalate from Baker was used without further purification. [2-Methyl-2-(3,5-di-*tert*-butyl-4-hydroxyphenyl)propyl]ammonium chloride,  $\text{ArOH}$ , was synthesized by a published procedure<sup>11</sup> and characterized by  $^1\text{H NMR}$ .

The molar absorption coefficient of  $\text{ArO}^*$  was determined by the reaction of excess  $\text{VO}^{2+}$  with a known amount of  $\text{H}_2\text{O}_2$  in the presence of  $\text{ArOH}$  according to eqs 4 and 5. Neither  $\text{VO}^{2+}$  nor  $\text{VO}_2^+$  reacts with  $\text{ArOH}$



to yield the  $\text{ArO}^*$  radical on the time scale used here. Therefore the molar absorptivity could be obtained from the absorbance change for the reaction of  $\text{VO}^{2+}$ ,  $\text{H}_2\text{O}_2$ , and  $\text{ArOH}$  at 400 nm. Experiments were conducted with  $\text{VO}^{2+}$  in excess over  $\text{H}_2\text{O}_2$ , and the absorbance changes were plotted against the concentration of  $\text{H}_2\text{O}_2$  added. The plot is linear at low  $[\text{H}_2\text{O}_2]$ , as expected, but deviates from the straight line at higher  $[\text{H}_2\text{O}_2]$  (Figure 1). From the initial linear portion we obtain  $\epsilon(\text{ArO}^*) = 1440 \pm 40 \text{ L mol}^{-1} \text{ cm}^{-1}$  at  $\lambda = 400 \text{ nm}$ . The deviation from linearity at higher  $[\text{H}_2\text{O}_2]$  can be accounted for by the known reaction<sup>12</sup> of  $\cdot\text{OH}$  with  $\text{H}_2\text{O}_2$ , eq 6. The  $\text{HO}_2^*/\text{O}_2^{\cdot-}$  produced is much less oxidizing than



$\cdot\text{OH}$  and is not expected to oxidize  $\text{ROH}$  to  $\text{RO}^*$ . Instead, superoxide will disproportionate to  $\text{O}_2$  and  $\text{H}_2\text{O}_2$ . The net effect of reaction 6 is to decrease the yield of  $\text{RO}^*$  at high  $[\text{H}_2\text{O}_2]$ , causing the curvature in Figure 1. A direct reaction between  $\text{RO}^*$  and  $\text{H}_2\text{O}_2$  could also play a role.<sup>13</sup> The electronic absorption spectrum of the 2,4,6-tri-*tert*-butylphenoxy radical has been measured by generating the radical by chemical oxidation and flash photolysis methods<sup>14a</sup> in hexane and by an electrochemical method<sup>14b</sup> in ethanol solution. In ethanol, the molar absorption coefficient at 400 nm was cited as  $\epsilon_{400\text{nm}} = 2.45 \times 10^3 \text{ L mol}^{-1} \text{ cm}^{-1}$ .<sup>14c</sup>

**Kinetics.** All the kinetic experiments were carried out at  $25.0 \pm 0.2$  °C by use of a Cary 219 or a Shimadzu UV-3101PC spectrophotometer equipped with an internal timer and a thermostated cell-holder. The kinetics were monitored directly at a wavelength giving the best absorbance

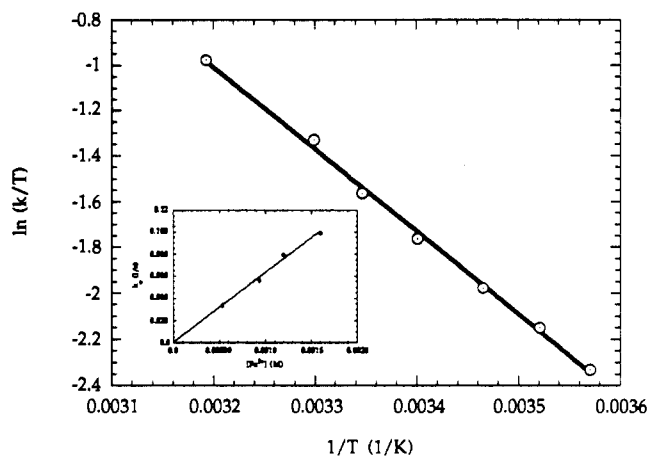


**Figure 2.** Plot of  $\ln(k/T)$  vs  $1/T$  according to transition state theory for the reaction of  $\text{CrOOH}^{2+}$  with  $\text{Fe}^{2+}$  at  $0.10 \text{ M H}^+$  and  $\mu = 0.42 \text{ M}$ . The inset is the plot of  $k_{\text{obs}}$  vs  $[\text{Fe}^{2+}]$  at  $25$  °C.

change. The absorbance ( $D$ )–time data were fitted to the equation  $D_t = D_\infty + (D_0 - D_\infty) \exp(-k_{\text{obs}}t)$  by use of the programs Spectracalc or Grafit.

The activation parameters for the reactions of  $\text{CrOOH}^{2+}$  with  $\text{Fe}^{2+}$  and of  $\text{CrO}^{2+}$  with  $\text{Fe}^{2+}$  were calculated from the Eyring equation. The kinetic measurements were conducted in the temperature ranges 6.9–40.0 and 5.1–25.0 °C, respectively.

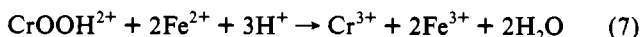
The kinetics of the reaction of  $\text{Fe}^{2+}$  with  $\text{ArO}^*$  were determined by allowing  $\text{H}_2\text{O}_2$  to react with a large excess of  $\text{Fe}^{2+}$  in the presence of  $\text{ArOH}$ . The rapid formation of  $\text{ArO}^*$  was followed by the slower reduction of  $\text{ArO}^*$  by  $\text{Fe}^{2+}$ . In a different experiment,  $\text{ArO}^*$  was prepared from  $\text{VO}^{2+}$ ,  $\text{H}_2\text{O}_2$ , and  $\text{ArOH}$ , as described earlier. The reaction of interest was then initiated by injecting  $\text{Fe}^{2+}$ . The agreement between the two methods was good and yielded  $k_{17} = 35.0 \pm 1.2 \text{ L mol}^{-1} \text{ s}^{-1}$ .

The stoichiometry of the reaction of  $\text{CrOOH}^{2+}$  with  $\text{Fe}^{2+}$  was calculated from the absorbance changes at 240 nm after the appropriate corrections for the absorption of  $\text{Fe}^{2+}$ ,  $\text{Ru}(\text{NH}_3)_6^{3+}$ , and  $\text{Cr}^{3+}$  were made.

The  $\text{CO}_2$  from the reaction of 0.05 mM  $\text{CrOOH}^{2+}$  with 0.15 mM  $\text{Fe}^{2+}$  in the presence of 5.7 mM oxalate at 0.10 M  $\text{H}^+$  was detected in the following way. After the reaction was completed (10 min), the  $\text{CO}_2$  was displaced from solution with a stream of argon and bubbled into a basic solution of  $\text{Ba}(\text{ClO}_4)_2$ , forming a fine precipitate of  $\text{BaCO}_3$ . A control experiment having all the same components except  $\text{CrOOH}^{2+}$  yielded no precipitate.

## Results

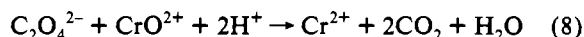
**Reaction with Iron(II).** Ferrous ion reduces  $\text{CrOOH}^{2+}$  according to the stoichiometry of eq 7, independent of  $[\text{H}^+]$  in the



range 0.10–0.50 M. The kinetics were conducted under pseudo-first-order conditions with  $\text{Fe}^{2+}$  in excess over  $\text{CrOOH}^{2+}$ . Typically, 0.06 mM  $\text{CrOOH}^{2+}$  was used to react with 0.8–4 mM  $\text{Fe}^{2+}$ . Experiments under Ar and  $\text{O}_2$  showed no difference in the kinetics or stoichiometry. The rate constant increased with the ionic strength. For example, at 0.10 M  $\text{H}^+$ , the rate constants of 48 and 81  $\text{L mol}^{-1} \text{ s}^{-1}$  were measured for the reactions at  $\mu = 0.10 \text{ M}$  and  $\mu = 0.50 \text{ M}$ , respectively.

Kinetic studies in the temperature range 6.9–40.0 °C yielded  $\Delta H^\ddagger = 30.0 \pm 0.7 \text{ kJ mol}^{-1}$  and  $\Delta S^\ddagger = -110 \pm 2 \text{ J mol}^{-1} \text{ K}^{-1}$  (Figure 2 and Table I).

**The Trapping of  $\text{CrO}^{2+}$ .** Oxalate ions were found previously<sup>15</sup> to reduce  $\text{CrO}^{2+}$  according to eq 8. The rate constant  $k_{\text{ox}}$  has a



- (10) Awtry, A. D.; Connick, R. R. *J. Am. Chem. Soc.* **1965**, *87*, 5026.  
 (11) Traylor, T. G.; Lee, W. A.; Stynes, D. V. *J. Am. Chem. Soc.* **1984**, *106*, 755.  
 (12) Christensen, H.; Sehested, K.; Corfitzen, H. *J. Phys. Chem.* **1982**, *86*, 1588.  
 (13) (a) Muller, E.; Mayer, R.; Narr, B.; Schick, A.; Scheffler, K. *Justus Liebig's Ann. Chem.* **1961**, *645*, 1. (b) Bickel, A. F.; Kooyman, E. C. *J. Chem. Soc.* **1953**, 3211.  
 (14) (a) Land, E. J.; Porter, G.; Strachan, E. *Trans. Faraday Soc.* **1961**, *57*, 1885. (b) Mauser, H.; Nickel, B. *Angew. Chem., Int. Ed. Engl.* **1965**, *4*, 354. (c) *DMS UV Atlas of Organic Compounds*; Butterworths, London, and Verlag Chemie, Weinheim, Germany, 1966; Vol. II, p D9/56.

- (15) Scott, S. L.; Bakac, A.; Espenson, J. H. *J. Am. Chem. Soc.* **1992**, *114*, 4205.

**Table I.** Activation Parameters for the Reductions of CrOOH<sup>2+</sup> and HOOH with Fe<sup>2+</sup>

peroxide	$k_{298}^a$	$\Delta H^\ddagger/\text{kJ mol}^{-1} b$	$\Delta S^\ddagger/\text{kJ mol}^{-1} \text{K}^{-1} b$
CrOOH <sup>2+</sup>	$48.4 \pm 0.7$	$30.0 \pm 0.7$	$-110 \pm 2$
HOOH	58	37	-86

<sup>a</sup> At  $\mu = [\text{H}^+] = 0.10 \text{ M}$ . <sup>b</sup> Values for H<sub>2</sub>O<sub>2</sub> were calculated from the data in: Hardwick, T. J. *Can. J. Chem.* **1957**, *35*, 428. Barb, W. G.; Baxendale, J. H.; George, P.; Hargrave, K. R. *Trans. Faraday Soc.* **1951**, *47*, 462. The data for CrOOH<sup>2+</sup> were obtained at  $\mu = 0.42 \text{ M}$  and  $[\text{H}^+] = 0.10 \text{ M}$ .

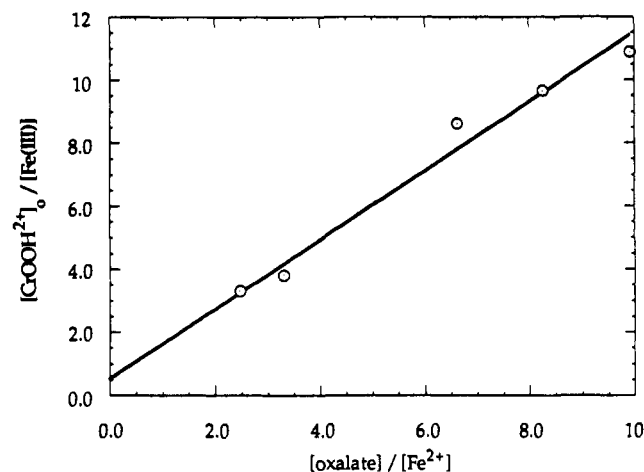
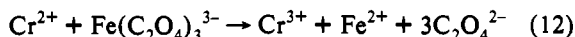
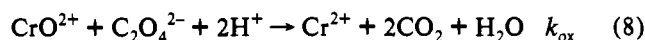
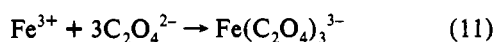
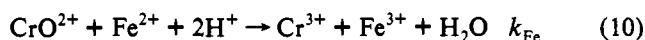
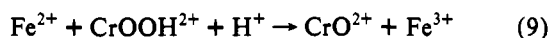


**Figure 3.** Plot of  $[\text{CrOOH}^{2+}]_0/[\text{Fe(III)}]$  as a function of  $[\text{oxalate}]/[\text{Fe}^{2+}]$  showing a linear relationship with an intercept of 0.52 and a slope of 1.08.  $[\text{CrOOH}^{2+}]_0 = (8.1\text{--}11.1) \times 10^{-5} \text{ M}$ ;  $[\text{Fe}^{2+}] = 2.52 \times 10^{-4} \text{ M}$ ;  $T = 25 \text{ }^\circ\text{C}$ ;  $\mu = [\text{H}^+] = 0.10 \text{ M}$ .

value of  $1.07 \times 10^3 \text{ L mol}^{-1} \text{ s}^{-1}$  at  $0.10 \text{ M H}^+$ , this being the composite value for  $\text{C}_2\text{O}_4^{2-}$  and  $\text{HC}_2\text{O}_4^-$  at this acidity.

The reaction of CrOOH<sup>2+</sup> with Fe<sup>2+</sup> in the presence of oxalate ions evolves considerable quantities of CO<sub>2</sub>. The kinetics are, however, unaffected by oxalate ions. A rate constant of  $k = 51.0 \pm 1.8 \text{ L mol}^{-1} \text{ s}^{-1}$  was measured in the presence of  $1.8 \text{ mM}$  oxalate, compared to  $48.4 \pm 0.7 \text{ L mol}^{-1} \text{ s}^{-1}$  in its absence. We assumed that the reaction takes place according to Scheme I and have measured the amounts of Fe(C<sub>2</sub>O<sub>4</sub>)<sub>3</sub><sup>3-</sup> produced as a function of the initial reactant concentrations.

#### Scheme I



By mixing known amounts of oxalate and Fe<sup>3+</sup> in a  $0.10 \text{ M H}^+$  solution, one can obtain a constant molar absorption coefficient only when the ratio  $[\text{oxalate}]/[\text{Fe}^{3+}]$  is larger than 40. On the other hand, to get a meaningful absorbance change in the experiments having Fe<sup>2+</sup>, oxalate, and CrOOH<sup>2+</sup>, the ratio  $[\text{oxalate}]/[\text{Fe}^{2+}]$  has to be kept within 10. These two requirements have limited the concentration variations in these experiments. The results are shown in Figure 3.

The yields of Fe(C<sub>2</sub>O<sub>4</sub>)<sub>3</sub><sup>3-</sup> produced are given in Table II. Although the reactions of Cr<sup>2+</sup> with CrO<sup>2+</sup> and CrOOH<sup>2+</sup> very likely have large rate constants, they were ignored in Scheme I, owing to the kinetic and concentration advantage of Fe(C<sub>2</sub>O<sub>4</sub>)<sub>3</sub><sup>3-</sup>.

**Table II.** Summary of the Trapping Experiments with Oxalate

$[\text{CrOOH}^{2+}]_0/10^{-5}$		$[\text{Fe}^{2+}]/\text{mM}$		$[\text{oxalate}]/\text{mM}$		$[\text{Fe(ox)}_3^{3-}]/10^{-5}$	
M						M	
11.5		1.08		0		22.7 <sup>a</sup>	
11.1		0.252		2.08		1.15	
11.1		0.252		0.833		2.92	
11.1		0.252		0.625		3.35	
8.4		0.506		0		16.6 <sup>a</sup>	
8.1		0.252		1.67		0.934	
8.1		0.252		2.50		0.759	

<sup>a</sup> Calculated from the absorbance change at 240 nm.

The fact that three different oxalate species were present in solution ( $\text{C}_2\text{O}_4^{2-}$ ,  $\text{HC}_2\text{O}_4^-$ , and  $\text{H}_2\text{C}_2\text{O}_4$ ) was ignored since all of the experiments were carried out at a constant  $[\text{H}^+]$  of  $0.10 \text{ M}$ .

The presence of oxalate has a profound effect on the reaction. The total amount of Fe<sup>3+</sup> produced in the absence of oxalate is  $0.227 \text{ mM}$ , i.e. close to twice the amount of initial  $[\text{CrOOH}^{2+}]$  ( $0.115 \text{ mM}$ ); this factor of 2 is expected from eqs 9–11. Even a small amount of oxalate ( $0.625 \text{ mM}$ ) drastically reduces the amount of Fe(III) found ( $0.0335 \text{ mM}$ ) due to the participation of reactions 8 and 12. In the presence of  $2.5 \text{ mM}$  oxalate, the amount of Fe(III) is only 5% of that found in the absence of oxalate.

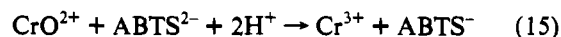
According to Scheme I the yield of Fe(C<sub>2</sub>O<sub>4</sub>)<sub>3</sub><sup>3-</sup> is related to the relative concentrations of  $[\text{Fe}^{2+}]$  and oxalate (eqs 13 and 14).

$$[\text{Fe(ox)}_3^{3-}]_\infty = [\text{CrOOH}^{2+}]_0 + [\text{CrOOH}^{2+}]_0 \frac{k_{\text{Fe}}[\text{Fe}^{2+}] - k_{\text{ox}}[\text{C}_2\text{O}_4^{2-}]}{k_{\text{Fe}}[\text{Fe}^{2+}] + k_{\text{ox}}[\text{C}_2\text{O}_4^{2-}]} \quad (13)$$

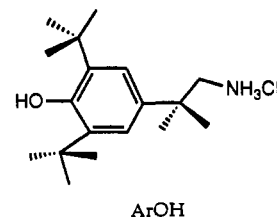
$$\frac{[\text{CrOOH}^{2+}]_0}{[\text{Fe}(\text{C}_2\text{O}_4)_3^{3-}]_\infty} = 0.5 + \frac{k_{\text{ox}}[\text{C}_2\text{O}_4^{2-}]}{2k_{\text{Fe}}[\text{Fe}^{2+}]} \quad (14)$$

The data fit the proposed scheme well, as illustrated by the plot of the left-hand side of eq 14 against the ratio  $[\text{oxalate}]/[\text{Fe}^{2+}]$ , Figure 3. The values of the intercept and slope are  $0.58 \pm 0.05$  and  $1.0 \pm 0.1$ , respectively. According to the proposed scheme, the slope represents the ratio of the rate constants for the reduction of CrO<sup>2+</sup> by oxalate and Fe<sup>2+</sup>. After the substitution for  $k_{\text{ox}}$ , the value of  $k_{\text{Fe}} = 500 \text{ L mol}^{-1} \text{ s}^{-1}$  is obtained. This rate constant applies to the reaction of (oxalato)iron(II) complexes with the chromyl ion; it is not the same as that reported later for the reaction of Fe(H<sub>2</sub>O)<sub>6</sub><sup>2+</sup> with the chromyl ion.

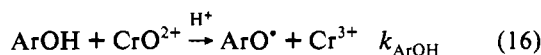
We attempted to use ABTS<sup>2-</sup> as a trap for CrO<sup>2+</sup> (eq 15),<sup>15</sup> but quantitative determinations were thwarted by the side reaction between the product, Fe<sup>3+</sup>, and ABTS<sup>2-</sup> that also yields ABTS<sup>-</sup>.



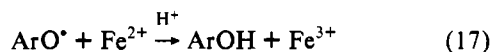
To confirm the formation of the chromyl intermediate a water-soluble phenol, [2-methyl-2-(3,5-di-*tert*-butyl-4-hydroxyphenyl)propyl]ammonium chloride, ArOH, was also used as a trap.



It was shown independently that CrO<sup>2+</sup> reacts with ArOH to yield ArO<sup>\*</sup>, an aryloxy radical that is persistent and reasonably intensely colored ( $\epsilon_{400} = 1.44 \times 10^3 \text{ L mol}^{-1} \text{ cm}^{-1}$ ) (eq 16). Controls showed that neither the separate reactants nor the spent reaction solution generated ArO<sup>\*</sup> upon addition of ArOH. The CrOOH<sup>2+</sup>-



$\text{Fe}^{2+}$  reaction, on the other hand, when conducted with ArOH added, did yield  $\text{ArO}^*$ . Unfortunately, the spectrum of  $\text{ArO}^*$  faded with time owing to the subsequent reduction of  $\text{ArO}^*$  by  $\text{Fe}^{2+}$  (eq 17), for which we have determined independently the



rate constant  $k_{17} = 35 \text{ L mol}^{-1} \text{ s}^{-1}$ . As expected, the higher the ratio  $[\text{Fe}^{2+}]/[\text{ArOH}]$ , the faster the disappearance of  $\text{ArO}^*$  formed in reaction 16. The ratio of the yield of  $\text{Fe}^{3+}$  ( $=[\text{CrOOH}^{2+}]_0 - [\text{ArO}^*]_\infty$ ) and  $[\text{ArO}^*]_\infty$  is predicted to be a linear function of the ratio of the concentrations of the competing reagents (eq 18).

$$\frac{[\text{CrOOH}^{2+}]_0 - [\text{ArO}^*]_\infty}{[\text{ArO}^*]_\infty} = \frac{k_{\text{Fe}}[\text{Fe}^{2+}]}{k_{\text{ArOH}}[\text{ArOH}]} \quad (18)$$

The absorbance changes at 400 nm could not be used to determine quantitatively the amounts of  $\text{ArO}^*$  produced, because of the side reaction of  $\text{ArO}^*$  with  $\text{Fe}^{2+}$ , eq 17. Only an estimate of  $k_{\text{Fe}}/k_{\text{ArOH}} \sim 37$  was obtained. When solutions of authentic  $\text{CrO}^{2+}$  were added to a mixture of  $\text{Fe}^{2+}$  and ArOH, the yield of  $\text{ArO}^*$  corresponded to  $k_{\text{Fe}}/k_{\text{ArOH}} = 21$  (Figure 4). The two values, 37 and 21, are reasonably close, given that the time scales for the two experiments differ appreciably. In the former case,  $\text{CrOOH}^{2+}$  and  $\text{Fe}^{2+}$  react over a period of approximately 10 min to yield the chromyl ion, which is then rapidly trapped by ArOH. During this time  $\text{Fe}^{2+}$  reduces some of the  $\text{ArO}^*$  formed, which thus escapes detection. The reaction between the chromyl ion and ArOH is, of course, the rapid trapping step in the reaction between  $\text{CrOOH}^{2+}$  and  $\text{Fe}^{2+}$ . When it occurs independently, it takes only a few seconds. The yield of  $\text{ArO}^*$  is thus nearly quantitative, and the determined ratio  $k_{\text{Fe}}/k_{\text{ArOH}}$  smaller. The reasonable agreement between the two values supports our contention that  $\text{CrO}^{2+}$  is the intermediate in the reaction of  $\text{CrOOH}^{2+}$  with  $\text{Fe}^{2+}$ . A more detailed analysis is given in the Discussion.

Direct kinetic measurements were performed on the reaction of  $\text{Fe}^{2+}$  with  $\text{CrO}^{2+}$  in the absence of oxalate. For these experiments,  $\text{CrO}^{2+}$  was prepared by oxidation of  $\text{Cr}^{2+}$  with  $\text{Tl(III)}$  to avoid the side reaction of  $\text{Fe}^{2+}$  with  $\text{CrO}_2^{2+}$  (a natural impurity in solutions of  $\text{CrO}^{2+}$  that are prepared from  $\text{O}_2$  and  $\text{Cr}^{2+}$ ). Without oxalate, the reaction of  $\text{Tl(III)}$  with  $\text{Fe}^{2+}$  was slow and did not interfere with the reaction of  $\text{CrO}^{2+}$  with  $\text{Fe}^{2+}$ . Figure 5 shows the plot of  $k_{\text{obs}}$  versus  $[\text{Fe}^{2+}]$  and the Eyring plot for this reaction. The activation parameters  $\Delta H^\ddagger = 28.3 \pm 1.8 \text{ kJ mol}^{-1}$  and  $\Delta S^\ddagger = -81 \pm 6 \text{ J K}^{-1} \text{ mol}^{-1}$  were obtained. The rate constant is  $3800 \text{ L mol}^{-1} \text{ s}^{-1}$  at  $25^\circ\text{C}$  and  $0.10 \text{ M H}^+$ , which is significantly larger than the value extracted from the competition experiments with oxalate. However, the presence of a strongly coordinating ligand, such as oxalate, may have changed the nature of the metal ions involved. The value of the rate constant for the  $\text{CrO}^{2+}/\text{Fe}^{2+}$  reaction in the presence of oxalate is thus needed. Unfortunately, the determination of this rate constant was not successful because of the interference from side reactions. As mentioned earlier, the  $\text{CrO}^{2+}$  prepared from  $\text{Cr}^{2+}$  and  $\text{O}_2$  contains significant amounts of  $\text{CrO}_2^{2+}$ , which also reacts with  $\text{Fe}^{2+}$  and thus interferes with the reaction of interest. When  $\text{CrO}^{2+}$  was prepared from  $\text{Cr}^{2+}$  and  $\text{Tl(III)}$ , the reaction of excess  $\text{Tl(III)}$  with  $\text{Fe}^{2+}$  in the presence of oxalate interfered with the measurement of the  $\text{CrO}^{2+}/\text{Fe}^{2+}$  reaction.

The reported rate constants for the reaction of  $\text{H}_2\text{O}_2$  with  $\text{Fe}^{2+}$

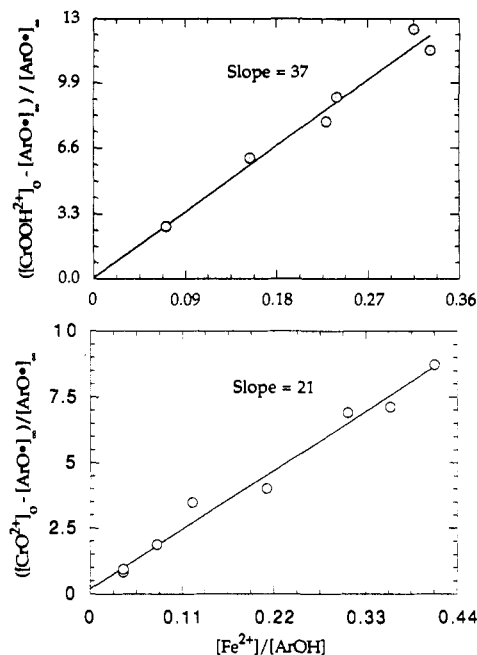


**Figure 4.** Linear relationship of the product distribution,  $([\text{CrOOH}^{2+}]_0 - [\text{ArO}^*]_\infty)/[\text{ArO}^*]_\infty$  or  $([\text{CrO}^{2+}]_0 - [\text{ArO}^*]_\infty)/[\text{ArO}^*]_\infty$ , vs the ratio  $[\text{Fe}^{2+}]/[\text{ArOH}]$  according to eq 18.  $T = 25^\circ\text{C}$ ;  $\mu = [\text{H}^+] = 0.10 \text{ M}$ .

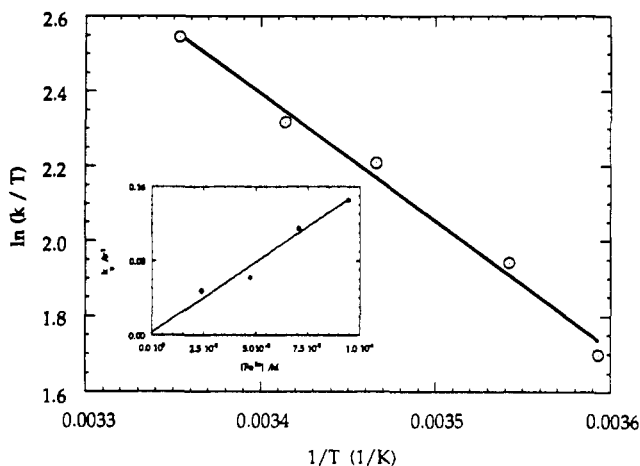


**Figure 5.** Eyring plot for the reaction of  $\text{CrO}^{2+}$  with  $\text{Fe}^{2+}$ . The inset is the plot of  $k_{\text{obs}}$  versus  $[\text{Fe}^{2+}]$  at  $25^\circ\text{C}$  ( $\mu = [\text{H}^+] = 0.10 \text{ M}$ ).

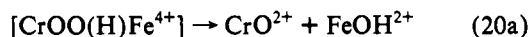
cover a rather wide range,  $40\text{--}80 \text{ L mol}^{-1} \text{ s}^{-1}$ .<sup>16</sup> We have therefore redetermined this rate constant and obtained a value of  $58 \text{ L mol}^{-1} \text{ s}^{-1}$  in  $0.10 \text{ M HClO}_4$ , in good agreement with some of the reported data<sup>16c-e</sup> (Table I).

## Discussion

**Mechanism.** As shown in Table I, the reactions of  $\text{Fe}^{2+}$  with  $\text{H}_2\text{O}_2$  and  $\text{CrOOH}^{2+}$  have strikingly similar rate constants and activation parameters. The salt effects differ, in agreement with expectations based on the charge types involved. The reaction with  $\text{H}_2\text{O}_2$  is unaffected by changes in ionic strength, whereas that with  $\text{CrOOH}^{2+}$  shows a positive salt effect. Indirectly, this ionic strength effect also serves as evidence that these are indeed two different reactions. Given that the rate constants at  $\mu = 0.10 \text{ M}$  are comparable (see Table I), it is important to be able to ascertain that reaction 7 is indeed a genuine reaction of  $\text{Fe}^{2+}$  with  $\text{CrOOH}^{2+}$ , and not that of  $\text{Fe}^{2+}$  with  $\text{H}_2\text{O}_2$  formed by decomposition of  $\text{CrOOH}^{2+}$ .

(16) (a) Walling, C. *Acc. Chem. Res.* **1975**, *8*, 125. (b) Wells, C. F.; Salam, M. A. *Trans. Faraday Soc.* **1967**, *63*, 620. (c) Hardwick, T. J. *Can. J. Chem.* **1957**, *35*, 428. (d) Barb, W. G.; Baxendale, J. H.; George, P.; Hargrave, K. R. *Trans. Faraday Soc.* **1951**, *47*, 462. (e) Po, H. N.; Sutin, N. *Inorg. Chem.* **1968**, *7*, 621.

Since reactions of  $\text{H}_2\text{O}_2$  with transition metal complexes require a precoordination of the peroxide to the metal, the kinetics of redox reactions are a function of both the reduction potentials and the rates of ligand substitution. From the data in Table I, we infer that the reaction of  $\text{CrOOH}^{2+}$  with  $\text{Fe}^{2+}$  also proceeds by an inner-sphere mechanism, eq 19. The binuclear intermediate  $\text{CrOO}(\text{H})\text{Fe}^{2+}$  can then cleave in either a one-electron (eq 20a) or a two-electron process (eq 20b). Both pathways are consistent with the kinetics and stoichiometry, and both feature a metal-oxo intermediate, the oxochromium(IV) or chromyl ion in eq 20a and an oxoiron(IV) or ferryl ion in eq 20b. The  $\text{Fe}^{2+}$  reduction of  $\text{FeO}^{2+}$ , produced in eq 20b, would take place in a reaction analogous to eq 10.



The trapping experiment with oxalate showed that an intermediate, reacting competitively with  $\text{Fe}^{2+}$  and  $\text{HC}_2\text{O}_4^-$ , is clearly involved. However, the unavailability of the rate constant for the reaction of  $\text{Fe}^{2+}$  with  $\text{CrO}^{2+}$  in the presence of oxalate makes it difficult to identify the intermediate unambiguously on the basis of the oxalate trapping experiments alone.

The model with  $\text{ArOH}$  as a trap predicts that the yield ratio should be a linear function of the ratio  $[\text{Fe}^{2+}]/[\text{ArOH}]$ , which passes through the origin. As shown in Figure 4, this is indeed the case.

The complete reaction scheme, taking into account all the competing and side reactions, is shown in Scheme II. Computer simulations based on this scheme and using known rate constants for the reactions of  $\text{CrO}^{2+}$  with  $\text{Fe}^{2+}$  ( $k = 3800 \text{ L mol}^{-1} \text{ s}^{-1}$ ) and  $\text{ArOH}$  ( $k = 240 \text{ L mol}^{-1} \text{ s}^{-1}$ )<sup>17</sup> were carried out. As shown in Figure 6, the calculated and experimental data agree well and support the assignment of  $\text{CrO}^{2+}$  as the intermediate. The possible oxidation of  $\text{CrOOH}^{2+}$  by  $\text{CrO}^{2+}$  was not considered in Scheme II. It is unlikely to occur in the presence of a large excess of  $\text{Fe}^{2+}$  and  $\text{ArOH}$  over  $\text{CrOOH}^{2+}$ .

The formation of  $\text{CrO}^{2+}$  rather than  $\text{FeO}^{2+}$  in reaction 20 indicates that the driving force for reaction 20a is greater than that for reaction 20b. This is consistent with the known trend of decreasing strength of the  $\text{M}=\text{O}$  bonds toward the right in the periodic table. Also,  $\text{Ce}(\text{IV})$  ( $E^\circ = 1.72 \text{ V}$ ) oxidizes  $\text{Cr}^{3+}$ , but not  $\text{Fe}^{3+}$ , supporting our contention that  $E^\circ(\text{Fe}^{\text{IV/III}}) > E^\circ(\text{Cr}^{\text{IV/III}})$ .

The similarity of the rate constants for the reductions of  $\text{CrOOH}^{2+}$  and  $\text{H}_2\text{O}_2$  by  $\text{Fe}^{2+}$  may be taken as additional support for the end-on ( $\eta^1$ ) structure for  $\text{CrOOH}^{2+}$ . It would appear

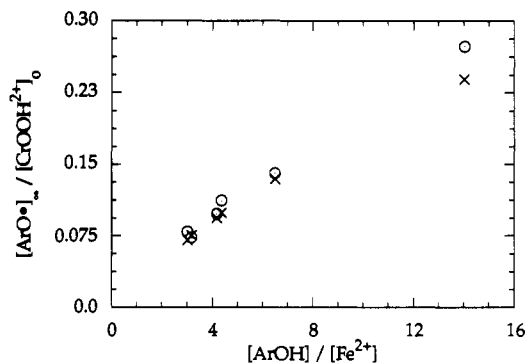
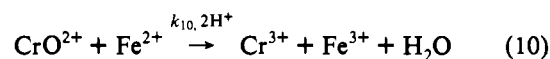
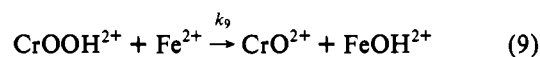


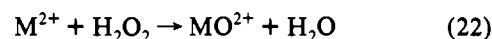
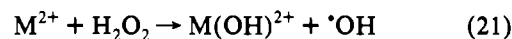
Figure 6. Experimental data (circles) and computer simulation (crosses, based on Scheme II) for the reaction of  $\text{CrOOH}^{2+}$  with  $\text{Fe}^{2+}$  in the presence of  $\text{ArOH}$ . The rate constants  $k_9$  ( $48 \text{ L mol}^{-1} \text{ s}^{-1}$ ),  $k_{10}$  ( $3800$ ),  $k_{\text{ArOH}}$  ( $240$ ), and  $k_{17}$  ( $35$ ) were set in the simulation at their independently measured values.

#### Scheme II



highly unlikely, although not impossible, that the  $\eta^2$  coordination of  $\text{H}_2\text{O}_2$  to chromium would not change its reactivity significantly.

The reactions of  $\text{H}_2\text{O}_2$  with both  $\text{Cr}^{2+}$  and  $\text{Fe}^{2+}$  (eq 21) yield OH radicals and metals in the 3+ oxidation state. If we accept that the potentials for both  $\text{M}^{\text{IV/III}}$  couples are significantly lower



than that for the  $\cdot\text{OH}/\text{H}_2\text{O}$  couple ( $+2.7 \text{ V}$ ),<sup>18</sup> then it becomes obvious that the thermodynamic products would be  $\text{MO}^{2+}$  and  $\text{H}_2\text{O}$  (eq 22). There is apparently no facile pathway for the observed, kinetic products ( $\text{MOH}^{2+}$  and  $\cdot\text{OH}$ ) to be converted to the thermodynamic ones during the short lifetime of  $\cdot\text{OH}$ .

**Acknowledgment.** This work was supported by a grant from the National Science Foundation (CHE-9007283). Some of the experiments were conducted with the use of the facilities of Ames Laboratory.

(17) Al-Ajlouni, A.; Bakac, A.; Espenson, J. H. Unpublished results.

(18) Wardman, P. *J. Phys. Chem. Ref. Data* **1989**, *18*, 1713.